Interactive Differential Segmentation of the Prostate using Graph-Cuts with a Feature Detector-based Boundary Term

Emmanouil Moschidis
emmanouil.moschidis@postgrad.manchester.ac.uk
Jim Graham
jim.graham@manchester.ac.uk

Imaging Science and
Biomedical Engineering
School of Cancer and
Enabling Sciences
The University of Manchester

Abstract

In this paper we present a modified boundary term for Graph-Cuts, which enables the latter to couple with feature detectors that return a confidence with respect to the detected image feature. Such detectors lead to improved localisation of boundaries in challenging images, which are often undetected by the implicit intensity-based edge detection scheme of the original method. This is particularly true for medical image segmentation, due to complex organ appearance, partial volume effect and weak intensity contrast at boundaries. The novel term is validated via its application to the differential segmentation of the prostate. The results demonstrate considerable improvement over classical Graph-Cuts of the Central Gland / Peripheral Zone separation when it is coupled with a SUSAN edge detector.

1 Introduction

In the last decade, Graph-Cuts has emerged as the standard interactive segmentation method due to its computational efficiency, precision and ability to achieve plausible outcomes with limited interaction. The segmentation is provided via the minimisation of its energy function, which consists of a weighted sum of a regional and a boundary term. The boundary term, which is often the only term in the energy function, is designed to align the segmentation boundary with intensity edges. This is achieved via its coupling with an implicit intensity-based edge detector. However, such an approach may be suboptimal for medical images, in which the boundaries may show intensity contrast that is weak, reduced by the partial volume effect, or characterised by texture changes.

In this paper we suggest a modification of the boundary term, which enables Graph-Cuts to couple with feature detectors that return a confidence with respect to the detected feature. This extends the original method and offers a wide selection of feature detectors that can recover boundaries, which are undetected by intensity-based edge detection. The novel term is validated via its application to the differential segmentation of the prostate, a challenging task for which model-based approaches have been employed [1]. The results demonstrate considerable improvement of the Central Gland/Peripheral Zone separation, when the new term is coupled with a SUSAN edge detector.

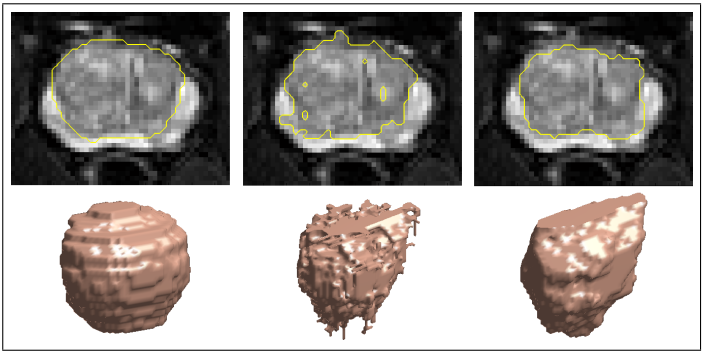

Figure 1: An axial slice of a T2 fat suppressed prostate MR image, with a line delineating the Central Gland (top) and a 3-D segmentation of the latter (bottom): (left) Ground Truth; (middle) Graph-Cuts; (right) modified Graph-Cuts coupled with SUSAN.

2 Methods

2.1 Dataset

The dataset used in this study consists of 22 3-D T2 fat suppressed Magnetic Resonance (MR) images of prostates from individuals with Benign Prostate Hyperplasia (BPH), a non cancerous enlargement of the prostate. Anatomically the prostate is divided into the Peripheral (PZ), the Central (CZ), the Transitional (TZ) and the fibromuscular zone [1]. In MR images only two regions are identified: the PZ and what is referred to as the Central Gland (CG) (Fig. 1), which consists of the remaining three zones. During treatment of BPH the physicians measure the volumes of the total prostate (TP) and the TZ, which is mostly enlarged due to the disease. TZ and CG are considered equivalent in this case.

Differential segmentation of the prostate is challenging due to the complex appearance of its regions. The CG appearance is textured and the borders between CG and PZ are often indistinguishable. The preprocessing of the dataset involved cropping the images close to the prostate, interpolating along the z-axis to allow for an iso-voxel resolution and normalising the voxel intensities to $[0,255]$. The ground truth was produced by averaging the manual segmentation of two experts.

2.2 Interactive Graph-Cuts

In interactive Graph-Cuts segmentation [2, 3] an image is represented as a graph. The user selects voxels that belong to the interior and the exterior of the object of interest, referred to as foreground and background seeds respectively. The optimal foreground/background boundary is then obtained via global minimisation of a cost function with min-cut/max-flow algorithms [4, 8]. Such a function is usually formulated as:

$$E(A) = \lambda \cdot R(A) + B(A) \tag{1}$$

where $R(A) = \sum_{p \in P} R_p(A_p)$, $B(A) = \sum_{\{p,q\} \in N} B_{\{p,q\}} \cdot \delta(A_p, A_q)$ and $\delta(A_p, A_q) = \begin{cases} 1 & \text{if } A_p \neq A_q \\ 0 & \text{otherwise.} \end{cases}$

$R(A)$ and $B(A)$ are the regional and boundary term of the energy function respectively. The

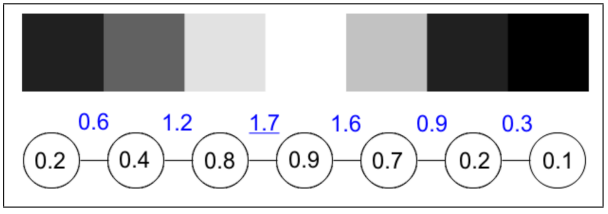

Figure 2: A 1-D example of the response of a feature detector and the equivalent 1-D graph. The edge weights are produced by summing the node values. The underlined figure represents the position of the cut, when the voxels on either side of the graph are connected to the source and the sink of the graph.

coefficient λ weighs the relative importance between the two terms. N contains all the unordered pairs of neighbouring voxels and A is a binary vector, whose components A_p, A_q assign labels to pixels p and q in P, respectively, on a given 2-D or 3-D grid.

The regional term assesses how well the intensity of a pixel p fits a known model of the foreground or the background. These models are either known a priori or estimated by the user input, when the latter is sufficient. Otherwise the regional term is weighted low relative to the boundary term or in practice $\lambda = 0$. This approach is followed in [2] as well as in this study. The boundary term encompasses the boundary properties of the configuration A, represented in the weighted graph. Each edge in this graph is usually assigned a high weight if the pixel intensity difference of its adjacent nodes is low and vice versa. The exact value of these weights is calculated with the following Gaussian function [3]:

$$B_{\{p,q\}} = K \cdot \frac{1}{dist(p,q)} \cdot \exp \frac{-(I_p - I_q)^2}{2\sigma^2} \tag{2}$$

where I_p and I_q are the intensities of two pixels p and q, and $dist(p,q)$ the euclidean distance between them. $dist(p,q)$ is set to 1 in case of equally spaced grids (iso-voxel volumes) when only the immediate neighbours are taken into account. Setting K to 1, leads to a Gaussian function with its peak equal to 1, which is useful for the normalisation of the graph weights. σ therefore is the only free parameter in Equation (2), which controls the full width at half maximum of the peak of the Gaussian function.

2.3 The Feature Detector Based Boundary Term

In order to couple Graph-Cuts with feature detectors, the following steps are followed: Firstly, since the raw response of most feature detectors [5],[12],[9] lies in the interval $[0,1]$, a Gaussian function as in [6] is used, where $\beta = \frac{1}{2\sigma^2}$. Secondly, the effect of the $|I_p - I_q|$ term is to locate the cut at points of high intensity difference. As we wish the cut to occur at maxima (ridges) in the feature output, we replace this term in the Gaussian function with $\frac{|R_p+R_q|}{2}$, where R_p and R_q is the response of the edge detector on pixel p and q respectively. Consequently we have:

$$B_{\{p,q\}} = \exp(-\varepsilon \cdot (R_p + R_q)^2) \tag{3}$$

where $\varepsilon = \frac{\beta}{4}$. Equation (3) describes the boundary term used in this study, which enables Graph-Cuts to couple with feature detectors. Figure 2 further illustrates the cut placement when the edge weights are calculated by summing the node values.

2.4 Feature Detectors

In this study the raw response of SUSAN (Smallest Univalue Segment Assimilated Nucleus) [12] was utilised to drive the Graph-Cuts segmentation. SUSAN in 3-D uses a spherical kernel, which defines a voxel neighbourhood. The value of the voxel at the center of the kernel is updated based on the detected intensity contrast between this voxel and its neighbours. A threshold is set by the user to determine the minimum contrast of features that will be detected. SUSAN's kernel-based operation enables it to respond to texture edges by taking into account the intensity variance of a voxel neighbourhood, which is a texture measure [7]. For this reason this detector was used for recovering the edges between CG and PZ. It was found useful to smooth the noisy output of the detector with a spherical kernel of radius equal to 7 that outputs the mean intensity of the voxels inside the kernel. The output was then normalised to $[0,1]$.

3 Experiments and Results

The validation experiment of this study consisted of segmentation of the Central Gland of the prostate from a dataset of 22 patients with BPH using Graph-Cuts and Graph-Cuts with the modified boundary term coupled with a SUSAN edge detector for the same computerised seed initialisation. The seeds were selected randomly to avoid any bias and in a computerised fashion to exclude human inconsistency from the evaluation process as in [11]. More specifically, 30 seeds were selected for the Central Gland, 30 for the Peripheral Zone and 30 for the Background, given the ground truth of these regions. The seeds were uniformly spread throughout the ground-truth volumes of interest. The reason for selecting 30 seeds is that we have previously observed [11] that this number of seeds is enough for the algorithm to converge to its best performance. For every image 30 different seed initialisations were used to allow for observations with statistical significance.

The two algorithms were optimised with respect to their free parameters, prior to the experiment. Graph-Cut's σ parameter was set to 0.8, SUSAN's threshold was set to 24 and ε was set to 120. The results (Table 1) showed a decrease of almost 20% in the volumetric difference between segmentation and ground truth, when the new algorithm was used. Fig. 1 shows an example segmentation that further illustrates the different outcome from original Graph-Cuts and our approach.

4 Concluding Remarks

In this paper a boundary term is presented, which enables Graph-Cuts to couple with feature detectors that return a confidence with respect to the detected image feature as in [10]. However, it can also make use of the raw response of detectors such as [5], [12], [9]. Its validation is performed via its application to the differential segmentation of the prostate. The results demonstrate considerable improvement of the CG/PZ separation when it is coupled with a SUSAN edge detector, for randomly selected seeds from the ground truth. The random selection of seeds was used to permit unbiased comparison between the algorithms. Our observation is that the results are further improved when the seeds are strategically selected by an expert. Given the fact that different detectors are appropriate for different domains, this enables Graph-Cuts to couple with the appropriate feature detector for a particular problem.

Method	Vol.Diff. (%)	Max.Dist (voxels)	Avg.Dist.(voxels)
GC	46.80 ± 7.24	10.69 ± 0.31	2.61 ± 0.11
GC+SUSAN	27.89 ± 3.84	7.35 ± 0.35	1.76 ± 0.07

Table 1: Mean differences from ground truth $\pm 1.96\times$ standard error across the 22 images, obtained from Graph-Cuts and Graph-Cuts+SUSAN segmentation for 30 randomly planted seeds.

5 Acknowledgements

This work is funded by the Biotechnology and Biological Sciences Research Council (BBSRC).

References

[1] P. D. Allen, J. Graham, D. C. Williamson, and C.E. Hutchinson. Differential segmentation of the prostate in MR images using combined 3D shape modelling and voxel classification. In *Proc. ISBI*, volume 1-3, pages 410–413, 2006.

[2] Y. Boykov and M.-P. Jolly. Interactive organ segmentation using graph cuts. *MICCAI*, (1935):276–286, 2000.

[3] Y. Boykov and M.-P. Jolly. Interactive graph cuts for optimal boundary and region segmentation of objects in N-D images. In *Proc. ICCV*, volume 1, pages 105–112, 2001.

[4] Y. Boykov and V. Kolmogorov. An experimental comparison of min-cut/max-flow algorithms for energy minimization in vision. *IEEE T-PAMI*, 26(9):1124–1137, 2004.

[5] J. Canny. A computational approach to edge detection. *IEEE T-PAMI*, 8(6):679–698, 1986.

[6] L. Grady. Random walks for image segmentation. *IEEE T-PAMI*, 28(11):1768–1783, 2006.

[7] R. M. Haralick. Statistical and structural approaches to texture. *Proc. IEEE*, 67(5): 786–804, 1979.

[8] V. Kolmogorov and R. Zabih. What energy functions can be minimized via graph cuts? *IEEE T-PAMI*, 26(2):147–159, 2004.

[9] P. Kovesi. Image features from phase congruency. *Videre*, 1(3):1–27, 1999.

[10] P. Meer and B. Georgescu. Edge detection with embedded confidence. *IEEE T-PAMI*, 23:1351–1365, 2001.

[11] E. Moschidis and J. Graham. A systematic performance evaluation of interactive image segmentation methods based on simulated user interaction. In *Proc. ISBI*, pages 928–931, 2010.

[12] S.M. Smith and M.J.Brady. SUSAN-A New approach to low level image processing. *IJCV*, 23(1):45–78, 1997.